Available online at www.sciencedirect.com
ScienceDirect
Trans. Nonferrous Met. Soc. China 29(2019) 1099−1106
Transactions of Nonferrous Metals Society of China
www.tnmsc.cn

Effect of iron valence on hydrothermal preparation of pyrochlore-type tungsten oxide

Qiu-sheng ZHOU, Min XIANG, Dong LI, Xiao-bin LI, Tian-gui QI, Zhi-hong PENG, Gui-hua LIU

School of Metallurgy and Environment, Central South University, Changsha 410083, China

Received 18 May 2018; accepted 27 February 2019

Abstract: Pyrochlore-type tungsten oxide (PTO), $WO_3 \cdot 0.5H_2O$, is an emerging material with very wide potential applications. The influences of iron valences and the additive amount of ferrous ion on tungsten crystallization ratio and the acceleration mechanism of ferrous ion were investigated when PTO was hydrothermally prepared in aqueous ammonium tungstate solution containing ammonium carbonate. The results show that ferrous ion can remarkably accelerate tungsten crystallization while both elemental iron and ferric ion have little influence on the crystallization. Moreover, the tungsten crystallization ratio increases with increasing the amount of ferrous ions added and reaches the maximum of about 60% with ferrous ion concentration of 16 g/L. FTIR analysis of the spent solution after PTO crystallization shows that ferrous ion can accelerate the conversion of WO_4 tetrahedral to WO_6 octahedron. Combined with XPS and XRD analyses of the hydrothermal product, the acceleration effect of ferrous ion on tungsten crystallization could basically be attributed to the increase in the interplanar spacing of PTO lattice caused by the incorporation of ferrous ion into PTO crystal lattice. The results presented is conducive to the efficient preparation of PTO powder and cleaner tungsten metallurgy.
Key words: pyrochlore-type tungsten oxide; ammonium tungstate solution; ferrous ion; crystallization; mechanism

1 Introduction

Pyrochlore-type tungsten oxide (PTO), $WO_3 \cdot 0.5H_2O$, is an important A-site defected layered perovskite oxide [1] with mesh pattern structure. As an emerging functional material with good performances, PTO is expected to be widely used in many fields such as photochromism, electrochromism, gasochromism, catalysis, humidity-sensing and battery materials [2−4]. On the other hand, PTO can also be used as a potential intermediate for preparing tungsten trioxide and tungsten powder in the cleaner extractive metallurgy of tungsten from scheelite and/or wolframite concentrates [5].

Considering the great potential applications of PTO, many researchers have studied its preparation by either soft chemical method [6] or hydrothermal method [7]. COUCOU and FIGLARZ [2] prepared PTO by dehydration of hydrated pyrochlore-type ammonium tungstates followed by ion exchange in acidic aqueous solutions. SCHAAK and MALLOUK [1] and KUDO et al [3] reported that PTO was successfully obtained by acid leaching of Aurivillus-type $Bi_2W_2O_9$ at about 25 °C for three days. However, the PTO preparation efficiency was very low due to its long duration. As for the hydrothermal method, REIS et al [8,9] and GUO et al [10] prepared PTO from acidified tungstate solution at pH less than 7.0. However, it was difficult to obtain high tungsten crystallization ratio. Later, LI et al [11] prepared PTO from aqueous alkaline sodium tungstate solution at 140 °C for 24 h at pH of 7.0−8.5 by adding organic acid and the tungsten crystallization ratio reached greater than 90%, indicating that PTO could also be prepared in the aqueous alkaline solution. But a relatively high temperature, long duration and expensive organic acid were required to achieve the high tungsten crystallization ratio from alkaline solution. Later, PENG et al [12] showed that iron species may have an acceleration effect on tungsten crystallization ratio when PTO was prepared from aqueous alkaline sodium tungstate solution using a steel bomb as the reactor. However, sodium impurity in the crystallization product was difficult to be removed. In order to avoid the presence of sodium in PTO, LI et al [13,14] have recently prepared PTO from aqueous ammonium tungstate solution instead of sodium tungstate solution in a steel bomb reactor, and detected a small quantity of iron present in PTO as well as the acceleration effect.

Foundation item: Project (51274243) supported by the National Natural Science Foundation of China
Corresponding author: Qiu-sheng ZHOU; Tel: +86-731-88830453; E-mail: qszhou@csu.edu.cn
DOI: 10.1016/S1003-6326(19)65018-1

Fortunately, tungsten-based alloys including element Fe have been drawn much attention because of their advantages of high melting point, high density, high elastic modulus, and resistance to neutron and gamma radiation [15−17]. Provided that iron species incorporate into and uniformly disperse in PTO lattice, the PTO with impurity of iron prepared from ammonium tungstate solution could probably be a desirable candidate for tungsten-based alloy preparation. So, it is very meaningful to further study the reaction behavior of iron in the hydrothermal preparation of PTO from aqueous alkaline ammonium tungstate solution. Under this circumstance, the influences of iron species on tungsten crystallization ratio and their reaction behaviors were investigated during the hydrothermal preparation of PTO from aqueous alkaline ammonium tungstate solution containing ammonium carbonate.

2 Experimental

2.1 Materials

Ammonium paratungstate ($(NH_4)_{10}H_2W_{12}O_{42}\cdot 4H_2O$, namely APT·$4H_2O$) used in this work was provided by Jiangxi Tungsten Industry Group Co., Ltd., China, and its purity meets the Grade one of the national standard GB/T 10116−2007. The other reagents used were analytically pure.

2.2 Preparation of aqueous ammonium tungstate solution

50% ammonia water was diluted with deionized water at a volume ratio of 1:3 to obtain diluted ammonia water. 300 g/L APT·$4H_2O$ was then added into the diluted ammonia water to hydrothermally synthesize aqueous ammonium tungstate solution by Reaction (1) in a sealed reactor at 120 °C for 2.5 h. The resultant was filtrated and the filtrate was used as the alkaline tungsten-bearing solution to prepare PTO. The WO_3 concentration in the filtrate was determined using the thiocyanate-spectrophotometric method [18].

$$5(NH_4)_2O\cdot 12WO_3\cdot 5H_2O+14NH_3\cdot H_2O=12(NH_4)_2WO_4+12H_2O \quad (1)$$

2.3 Preparation of PTO seed

Deionized water and $(NH_4)_{10}H_2W_{12}O_{42}\cdot 4H_2O$ (APT·$4H_2O$) with a liquid to solid mass ratio (L/S) of 1:1 were put into a 150 mL stainless-steel bomb, and then the sealed bomb was immersed in molten salts and rotated for a certain duration. The molten salt as the heating medium was preheated to a preset temperature with precision of 1 °C. After hydrothermal reaction, the bomb was taken out and cooled abruptly to room temperature by tap water. The resultant slurry was filtered and the cake was dried in an electro-thermostatic blast oven at 100 °C for 8 h to obtain transformation product used for XRD analyses.

2.4 PTO preparation

PTO seed hydrothermally transformed by APT·$4H_2O$ in Section 2.2, ammonium carbonate, and the synthesized aqueous ammonium tungstate solution were placed in a 150 mL stainless-steal autoclave which is specifically lined with polytetrafluoroethylene to eliminate the influence of iron probably introduced by the steel bomb. The additive amount of PTO seed was determined by the seed ratio of m_j/m_r as 3.0:1.0 [19], where m_j and m_r represent the mass of PTO seed and that of tungsten as $WO_3\cdot 0.5H_2O$ in the ammonium tungstate solution, respectively. Additionally, two zirconium balls with diameter of 5 mm were added to the autoclave to intensify agitation. To clarify the influence of impurity iron on the preparation of PTO, different iron species with different valences and dosages were simultaneously added into the autoclave. Subsequently, the sealed autoclave was immersed in a glycerol cell preheated at a preset temperature (precision of 1 °C) and rotated for a certain reaction time. During the rotation, the main hydrothermal reaction was shown in Eq. (2). When the reaction was completed, the autoclave was taken out from the cell and cooled abruptly to room temperature by tap water. After filtration of the resultant slurry, the obtained cake was washed several times by deionized water and then dried for further analyses, and the filtrate was used to determine WO_3 concentration in the spent solution.

$$(NH_4)_2WO_4+1.5H_2O=WO_3\cdot 0.5H_2O+2(NH_3\cdot H_2O) \quad (2)$$

Tungsten crystallization ratio, η (%), during the hydrothermal preparation of PTO from the solution was calculated by Eq. (3).

$$\eta=(\rho_0-\rho_t)/\rho_0\times 100\% \quad (3)$$

where ρ_0 and ρ_t denote tungsten concentration as WO_3 in tungstate solutions before and after hydrothermal reaction, respectively, g/L.

2.5 Analyses of hydrothermal product

Phase analysis of the hydrothermal product was performed on a Bruker X-ray diffractometer (D8-Advance, Germany) with Cu K_α monochromatic X-ray. The data were recorded for 2θ from 5° to 75° and 0.0085° of step size was taken at a scan rate of 1 (°)/min, and the current and voltage of the generator were respectively set at 30 mA and 40 kV. The FTIR spectra of tungstate solutions smeared on the surface of KBr plates were collected on a FTIR spectrometer (Nicolet 6700, USA) with 4 cm^{-1} resolution. X-ray photoelectron spectroscopy (XPS) measurements were conducted on a

K-alpha 1063 spectrometer (Thermo Fisher Scientific, USA) with monochromatic Al K_α as the excitation source.

3 Results and discussion

3.1 Preparation of PTO seed

Following Reaction (4), APT·$4H_2O$ was hydrothermally transformed to PTO. Figure 1 shows the XRD patterns of transformation products prepared at different hydrothermal transformation temperatures.

$$(NH_4)_{10}H_2W_{12}O_{42}\cdot 4H_2O+6H_2O=$$
$$12(WO_3\cdot 0.5H_2O)+10(NH_3\cdot H_2O) \quad (4)$$

As shown in Fig. 1, all the detected diffraction peaks are characteristic ones of APT·$4H_2O$ at temperature lower than 140 °C, and APT·$4H_2O$ gradually converts to PTO with increasing hydrothermal temperature. At 160 °C, there are distinct characteristic peaks of PTO as well as those of APT·$4H_2O$. When temperature is above 180 °C, there are no other diffraction peaks detected except those of PTO, meaning that APT·$4H_2O$ completely converts to PTO. Hence, the transformation products prepared at 200 °C for 6 h were used as PTO seed in the subsequent experiments.

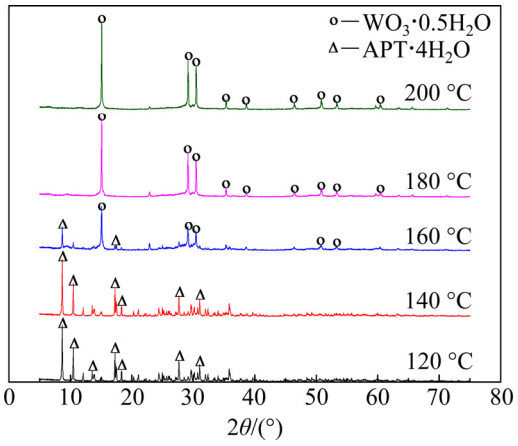

Fig. 1 XRD patterns of transformation products prepared at different hydrothermal temperatures (L/S 1:1, hydrothermal duration 6 h)

3.2 Influence of iron species on hydrothermal preparation of PTO in aqueous ammonium tungstate solution

3.2.1 Influence of iron valence on tungsten crystallization ratio

Aiming to examine the effect of iron valence on tungsten crystallization ratio, three iron species with different valences, i.e., iron powder, ferrous sulphate and ferric sulphate, were separately added into the hydrothermal system to examine the influence of iron valence on tungsten crystallization ratio. For convenient comparison, different iron species added contain the same amount of 16 g/L as element iron.

The experimental results listed in Table 2 show that tungsten crystallization ratios are respectively 25.45% and 26.61% with and without element iron added, indicating that zerovalent element iron has little influence on the tungsten crystallization ratio. However, the tungsten crystallization ratios reach 61.34% and 28.13% with adding heptahydrate ferrous sulphate and ferric sulphate, respectively, suggesting that trivalent iron can slightly accelerate the crystallization of tungsten while divalent iron has a remarkable acceleration effect on the crystallization.

Table 2 Influences of iron valences on tungsten crystallization ratio

Iron species	Additive amount designated by element iron/(g·L^{-1})	η/%
Blank	0	26.61
Iron powder	16	25.45
$FeSO_4\cdot 7H_2O$	16	61.34
$Fe_2(SO_4)_3$	16	28.13

$\rho(WO_3)$=220 g/L, seed ratio m_j/m_r=3.0:1.0, $\rho[(NH_4)_2CO_3]$=500 g/L, 130 °C, 12 h

3.2.2 Influence of additive amount of ferrous ion on tungsten crystallization ratio

As divalent iron ($FeSO_4\cdot 7H_2O$) has a remarkably positive effect on the crystallization of tungsten from the ammonium tungstate solution, the influence of the additive amount of ferrous ion on the tungsten crystallization was further studied. The added divalent iron increased from 0 to 20 g/L as element iron and the corresponding results are plotted in Fig. 2.

As shown in Fig. 2, the tungsten crystallization ratio increases gradually with the added ferrous ion amount less than 4 g/L, then grows rapidly in the range of

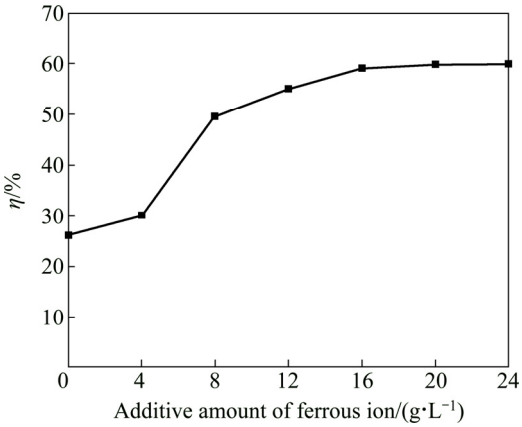

Fig. 2 Influence of additive amount of ferrous ion on tungsten crystallization ratio ($\rho(WO_3)$=220 g/L, seed ratio m_j/m_r=3.0:1.0, $\rho[(NH_4)_2CO_3]$=500 g/L, 130 °C, 12 h)

4−8 g/L, and subsequently rises slowly at 8−20 g/L. The tungsten crystallization ratio reaches about 60% with divalent iron concentration of 20 g/L. In other words, tungsten crystallization ratio increases with increasing the amount of ferrous ions added, but the acceleration effect becomes weaker with ferrous ion concentration greater than 16 g/L. This implies that the acceleration effect of divalent iron on the tungsten crystallization is not caused by the formation of ferrous tungstate through the direct reaction of ferrous iron with tungstate ions in the solution, and there is a certain underlying mechanism for the acceleration effect.

3.2.3 Influence of ferrous ion on morphology of hydrothermal product

The influence of ferrous ion on the morphology of hydrothermal product was further studied by SEM analysis. As shown in Fig. 3(a), the original crystal size of the hydrothermal product is ~1 μm at divalent iron concentration of 4 g/L. With the increase of the divalent iron concentration, the change in original crystal size is not distinct, whereas the agglomeration tendency among crystals is increasingly obvious (see Figs. 3(c)−(e)). When the ferrous ion content is at 20 g/L, the agglomerate size reaches greater than 5 μm (Figs. 3(d), (e)). This may be correlated to the rapid increase of the concentration of WO_6 octahedron caused by the conversion of WO_4 tetrahedral(see Section 3.3.1) when the divalent iron concentration increases rapidly. That is to say, along with the anion conversion of WO_4 into WO_6, the supersaturation of WO_6 anion in the solution increases and thus PTO precipitates more rapidly, thus enhancing agglomeration. As for the intrinsic dependence of PTO crystallization on the WO_6 anion, supersaturation is to be further investigated.

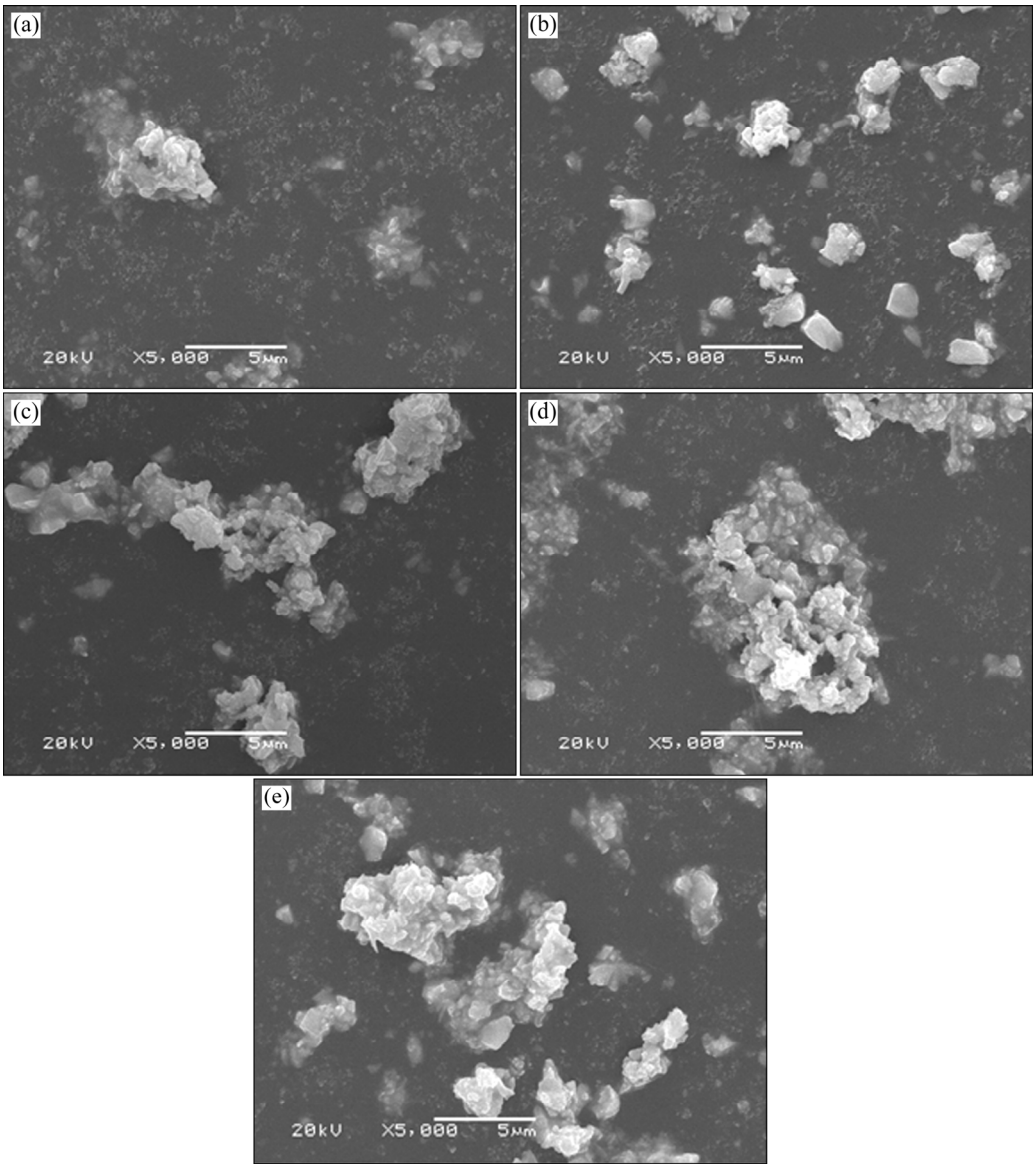

Fig. 3 SEM images of hydrothermal product with different additive amounts of ferrous ion ($\rho(WO_3)$=220 g/L, $\rho((NH_4)_2CO_3)$=500 g/L, seed ratio m_j/m_r=3.0:1.0, 130 °C, 12 h): (a) 4 g/L; (b) 8 g/L; (c) 12 g/L; (d) 16 g/L; (e) 20 g/L

3.3 Acceleration mechanism for tungsten crystallization

3.3.1 FTIR analysis of spent solution after PTO crystallization

The change of tungsten species in the spent solution after tungsten crystallization with different amounts of divalent iron added was explored by FTIR, and Fig. 4 shows the FTIR spectra with divalent iron concentration varying from 0−20 g/L. According to the study by WANG et al [20], the peak centered at 833 cm^{-1} corresponds to the absorption peak of WO_4 tetrahedron which makes up the tungstate ion, and the peak at 930 cm^{-1} is the absorption peak of WO_6 octahedron which is the structural unit of PTO. As shown in Fig. 4, the intensity of the absorption peak at 833 cm^{-1} decreases markedly with increasing the amount of ferrous iron added, while that at 930 cm^{-1} keeps almost stable slightly. Additionally, there is no remarkable change in the other absorption peaks corresponding to tungsten-bearing ions. This reveals that WO_4 tetrahedrals in the tungstate solution transform into WO_6 octahedrons which subsequently precipitate in the form of PTO with the increase of ferrous ion concentration, i.e., ferrous ion can accelerate the conversion of WO_4 tetrahedral to WO_6 octahedron, resulting in the rapid precipitation of PTO.

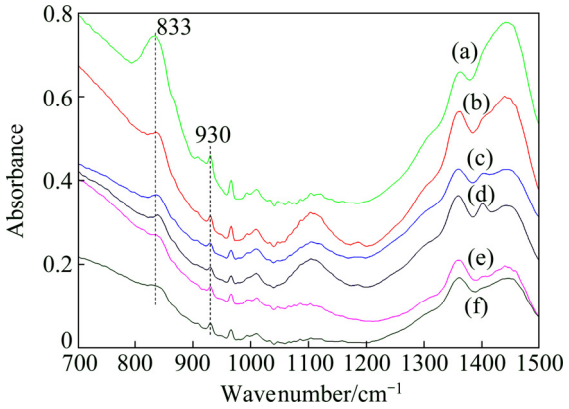

Fig. 4 FTIR spectra of spent solution of PTO crystallization with different divalent iron concentrations ($\rho(WO_3)$=220 g/L, $\rho((NH_4)_2CO_3)$=500 g/L, seed ratio m_j/m_r=3.0:1.0, 130 °C, 12 h): (a) 0 g/L; (b) 4 g/L; (c) 8 g/L; (d) 12 g/L; (e) 16 g/L; (f) 20 g/L

3.3.2 XPS measurement of hydrothermal product

In order to further explore the acceleration mechanism for tungsten crystallization by adding ferrous ion in the hydrothermal preparation of PTO, the hydrothermal product prepared by adding 16 g/L ferrous ions was employed to analyze its chemical composition, which shows that about 23 wt.% of iron quantitatively determined by ICP analysis enters into the hydrothermal product. Moreover, the chemical states of the elements of the product were examined by X-ray photoelectron spectroscopy (XPS) measurement to determine the iron valence and the interactions between iron and PTO. As shown in Fig. 5, the survey spectrum (Fig. 5(a)) of the product shows the peaks of of Fe 2p at 711.19 eV, W 4f at 35.76 eV and O 1s at 530.89 eV, confirming the presence of Fe, W and O elements in the surface structure of the product. The W 4f photoelectron spectrum (Fig. 5(c)) manifests W 4f (35.76 eV) and W 4f (37.88 eV), which is in agreement with the binding energy values of W^{6+}. With respect to Fe, the core-level Fe 2p photoelectron spectrum (Fig. 5(b)) reveals Fe $2p_{2/3}$ (709.19 eV) and Fe $2p_{1/3}$ (724.63 eV). However, for element Fe, as the binding energy values of its various forms are very close, the valence of element Fe cannot be determined directly from Fig. 5(b). Therefore, XPS spectrum peaks of Fe are further split to determine the existent form of iron in the hydrothermal product. As depicted in Fig. 6. the peaks of 710.2, 711.3, 712.4 and 713.6 eV correspond to ferric ion, while those of 708.3, 709.3 and 710.4 eV are assigned to ferrous ion. Moreover, the area of each peak was calculated (Table 3) to estimate the content of ferric and ferrous iron. As shown in Table 3, the ratio of total area of ferric ion peaks to that of ferrous iron peaks is about 42:58, meaning that approximate 60% of iron on the surface of the hydrothermal product still exists in the form of ferrous ion and about 40% of ferrous ion is oxidized into ferric ion during the hydrothermal preparation of PTO.

3.3.3 XRD analysis of hydrothermal products

On the basis of XPS analysis of the surface structure of the hydrothermal product, XRD analyses (Fig. 7) of the products were conducted to further find out the phase of iron species present in the product. As shown in Fig. 7, the main phase of the product is PTO when the ferrous ion content added increases from 0 to 20 g/L during the hydrothermal preparation of PTO. However, compared with the XRD pattern of the PTO obtained without adding ferrous iron during the hydrothermal preparation, an accompanying peak in low-angle direction appears closely adjacent to the characteristic peaks at approximate 30° of PTO, and its intensity seems to slightly increase with increasing the amount of ferrous ion added. According to the Bragg's law, an accompanying peak deviates in a low-angle direction, which is caused by the enlargement of interplanar spacing [21]. On the other hand, the three-dimensional channels among the layers of PTO facilitate the exchange of cations. Combining with the aforementioned FTIR and XPS results, we could deduce that, the added ferrous ion during the hydrothermal reaction may incorporate into PTO crystal lattice most probably by lattice substitution of tungsten by iron, causing the increase of PTO interplanar spacing. Subsequently, some

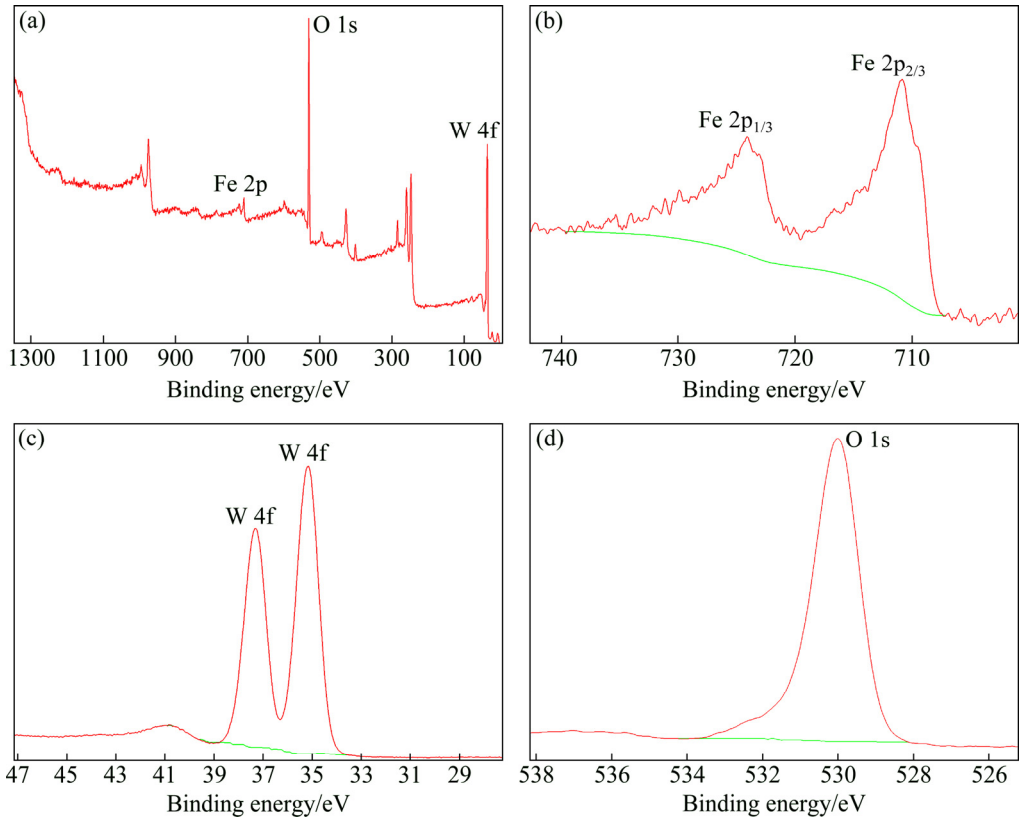

Fig. 5 XPS spectra of hydrothermal product obtained by adding 16 g/L ferrous iron ($\rho(WO_3)$=220 g/L, $\rho((NH_4)_2CO_3)$=500 g/L, seed ratio m_j/m_r=3.0:1.0, 130 °C, 12 h): (a) Survey spectrum; (b) Fe 2p scan; (c) W 4f scan; (d) O 1s scan

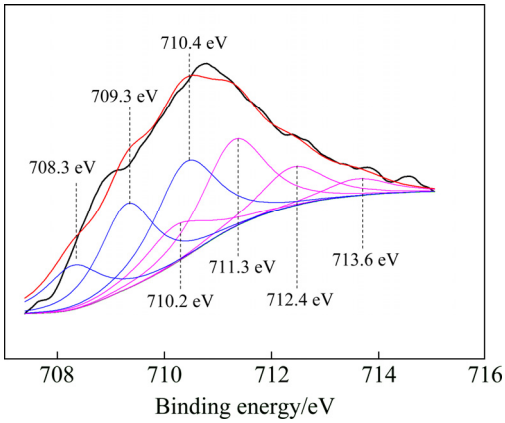

Fig. 6 Split XPS spectra of element Fe on surface of hydrothermal product

Table 3 Each peak area of XPS spectra of element Fe in product

Binding energy/eV	Peak area
710.2	1134.5
711.3	2177.8
712.4	1185.3
713.6	551.6
708.3	1235.7
709.3	2492.5
710.4	3215.9

physicochemical properties of the crystallization product change to some extent and ultimately accelerate the crystallization of tungsten in the solution. To verify this deduction, the lattice parameters (Table 4) of each hydrothermal product in Fig. 7 were determined. From Table 4, we can see that the lattice parameter of the product obtained without adding ferrous ion is 1.02693 nm which is very close to that of 1.0270 nm of the standard cubic PTO. With the increment of added ferrous ion, the lattice parameter gradually increases from 1.02723 to 1.02813 nm. Therefore, the acceleration of PTO crystallization by introducing ferrous ion during its hydrothermal preparation could be basically attributed to the incorporation of ferrous ion into the PTO lattice.

In addition, when the additive amount of ferrous ion reaches 20 g/L, the characteristic peaks of ferriferrous oxide can be detected distinctly. Therefore, a conclusion may be drawn that the ferric ion in the hydrothermal products exists in the form of ferriferrous oxide. Theoretically, the mass ratio of ferric ion to ferrous ion in a pure ferriferrous oxide should be about 67:33. However, the mass ratio for the product obtained by adding 16 g/L ferrous iron is about 42:58 by the XPS analysis, which further proves that partial ferrous ions incorporate into PTO lattice during the hydrothermal preparation.

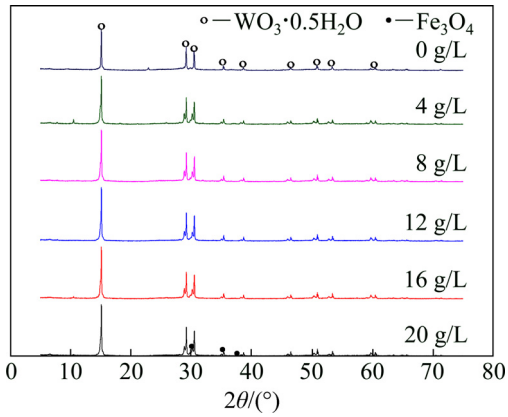

Fig. 7 XRD patterns of hydrothermal products obtained by adding different amounts of Fe^{2+} ($\rho(WO_3)$=220 g/L, seed ratio m_j/m_r=3.0:1.0, $\rho((NH_4)_2CO_3)$=500 g/L, 130 °C, 12 h)

Table 4 Lattice parameters of hydrothermal products at different additive amounts of ferrous ion

Ferrous ion amount/(g·L^{-1})	Lattice parameter/nm
0	1.02693
4	1.02723
8	1.02748
12	1.02774
16	1.02792
20	1.02813

$\rho(WO_3)$=220 g/L, $\rho((NH_4)_2CO_3)$=500 g/L, seed ratio m_j/m_r=3.0:1.0, 130 °C, 12 h

4 Conclusions

(1) Ferrous ion can markedly accelerate tungsten crystallization ratio in the hydrothermal preparation of PTO from aqueous ammonium tungstate/carbonate solution, while both element iron and ferric ion have little influence on the tungsten crystallization.

(2) The tungsten crystallization ratio increases with increasing ferrous ion concentration and reaches 61.34% at ferrous ion concentration of 16 g/L, afterwards, the acceleration effect becomes weak.

(3) The acceleration effect of ferrous ion on tungsten crystallization during the hydrothermal preparation of PTO could basically be attributed to the increase in the PTO interplanar spacing caused by the incorporation of partial ferrous ion into PTO crystal through lattice substitution. Additionally, partial ferrous ion is oxidized and exists in ferriferous oxide in the hydrothermal product.

References

[1] SCHAAK R E, MALLOUK T E. Exfoliation of layered rutile and perovskite tungstates [J]. Chemical Communications, 2002, 21(7): 706−707.

[2] COUCOU A, FIGLARZ M. A new tungsten oxide with 3D tunnels: WO_3 with the pyrochlore-type structure [J]. Solid State Ionics, 1988, 28−30: 1762−1765.

[3] KUDO M, OHKAWA H, SUGIMOTO W, KUMADA N, LIU Z, TERASAKI O, SUGAHARA Y. A layered tungstic acid $H_2W_2O_7·nH_2O$ with a double-octahedral sheet structure: Conversion process from an Aurivillius phase $Bi_2W_2O_9$ and structural characterization [J]. Inorganic Chemistry, 2003, 42(14): 4479−4484.

[4] ZHOU Q S, CHEN Y K, LI X B, QI T G, PENG Z H, LIU G H. Preparation and electrochromism of pyrochlore-type tungsten oxide film [J]. Rare Metals, 2018, 37(7): 604−612.

[5] SHEN L T，LI X B，ZHOU Q S，PENG Z H, LIU G H, QI T G, TASKINEN P. Sustainable and efficient leaching of tungsten in ammoniacal ammonium carbonate solution from the sulfuric acid converted product of scheelite [J]. Journal of Cleaner Production, 2018, 197: 690−698.

[6] SHEN L T，LI X B，ZHOU Q S，PENG Z H, LIU G H, QI T G, TASKINEN P. Wolframite conversion in treating a mixed wolframite-scheelite concentrate by sulfuric acid [J]. JOM, 2018, 70(2): 161−167.

[7] GÉRAND B, SEGUIN L. The soft chemistry of molybdenum and tungsten oxides: A review [J]. Solid State Ionics, 1996, 84(3−4): 199−204.

[8] REIS K P, RAMANAN A, WHITTINGHAM M S. Hydrothermal synthesis of sodium tungstates [J]. Chemistry of Materials, 1990, 2(3): 219−221.

[9] REIS K P, PRINCE E, WHITTINGHAM M S. Rietveld analysis of $Na_xWO_{3+x/2}·yH_2O$, which has the hexagonal tungsten bronze structure [J]. Chemistry of Materials, 1992, 4(2): 307−312.

[10] GUO J, LI Y J, WHITTINGHAM M S. Hydrothermal synthesis of electrode material: Pyrochlore tungsten trioxide film [J]. Journal of Power Sources, 1995, 54(2): 461−464.

[11] LI X B, LI J P, ZHOU Q S, PENG Z H, LIU G H, QI T G. Direct hydrothermal precipitation of pyrochlore-type tungsten trioxide hemihydrate from alkaline sodium tungstate solution [J]. Metallurgical and Materials Transactions B, 2012, 43(2): 221−228.

[12] PENG Z H, WU X, ZHOU Q S, YU X J, QI T G, LIU G H, LI X B. Preparation of ultrafine pyrochlore-type tungsten trioxide powder by hydrothermal method and its characterization [J]. The Chinese Journal of Nonferrous Metals, 2012, 22(2): 579−584. (in Chinese)

[13] LI X B, GAO C H, ZHOU J, ZHOU Q S, QI T G, LIU G H, PENG Z H. Dissolving behavior of ammonium paratungstate in $(NH_4)_2CO_3$−$NH_3·H_2O$−H_2O system [J]. Transactions of Nonferrous Metals Society of China, 2018, 28(7): 1456−1464.

[14] LI X B, SHEN L T, TONG X Y, QI T G, ZHOU Q S, LIU G H, PENG Z H. Thermodynamic modeling on reaction behaviors of silicates in $(NH_4)_2WO_4$−$(NH_4)_2CO_3$−NH_3−H_2O system [J]. Transactions of Nonferrous Metals Society of China, 2018, 28(11): 2342−2350.

[15] FAN J L, HUANG B Y, WANG D L, QU X H, ZHANG C F. Preparation technology of nanometer size refractory high density tungsten based alloy composite powders [J]. Rare Metal Materials and Engineering, 2001, 30(6): 401−405. (in Chinese)

[16] MA Y Z, ZHAO Y X, LIU W S, ZHANG J J. Research on viscosity and rheological properties of tungsten-based alloy PEM feed [J]. Rare Metal Materials and Engineering, 2010, 39(11): 1979−1983. (in Chinese)

[17] DAS J, KIRAN U R, CHAKRABORTY A, PRASAD N E. Hardness and tensile properties of tungsten based heavy alloys prepared by liquid phase sintering technique [J]. International Journal of Refractory Metals & Hard Materials, 2009, 27: 577−583.

[18] RAMOS-DELGADO N A, GRACIA-PINILLA M A, MAYA-TREVINO L, HINOJOSA-REYES L, GUZMAN-MAR J L, HERNANDEZ-REMIREZ A. Solar photocatalytic activity of TiO_2

modified with WO_3 on the degradation of an organophosphorus pesticide [J]. Journal of Hazardous Materials, 2013, 263: 36−44.
[19] LI Dong. Hydrothermal precipitation of pyrochlore-type tungsten trioxide from ammonium tungstate solution and effect of iron [D]. Changsha: Central South University, 2017. (in Chinese)
[20] WANG Y W, WANG Z D, CHENG H B. Structure and spectrum of the novel laser crystal Yb: $KY(WO_4)_2$ [J]. Acta Physica Sinica, 2006, 55(9): 4803−4808. (in Chinese)
[21] YU Q Z. X-ray powder diffraction phase analysis of full spectrum fitting [D]. Qufu: Qufu Normal University, 2002. (in Chinese)

铁的价态对水热制备焦绿石型氧化钨的影响

周秋生，项 敏，李 栋，李小斌，齐天贵，彭志宏，刘桂华

中南大学 冶金与环境学院，长沙 410083

摘 要：焦绿石型氧化钨是一种具有广泛潜在用途的新兴材料。研究从钨酸铵−碳酸铵溶液中水热制备焦绿石型氧化钨过程中铁的价态和亚铁离子添加量对钨结晶率的影响，重点研究亚铁离子促进钨结晶过程的机理。结果表明，亚铁离子能显著促进钨的结晶过程，而单质铁和三价铁离子的影响甚微；钨结晶率随亚铁离子添加量的增加而升高，当亚铁离子浓度为 16 g/L 时，钨结晶率达到最大值~60%。结晶母液的红外光谱(FTIR)分析表明，亚铁离子能促进溶液中 WO_4 四面体向 WO_6 八面体转变；结合结晶产物的 X 射线光电子能谱(XPS)和 X 射线衍射(XRD)分析，亚铁离子对钨结晶的促进作用可归因于亚铁离子嵌入焦绿石型氧化钨晶格而导致其面间距的增加。研究结果有助于焦绿石型氧化钨粉体的高效制备和钨的清洁生产。

关键词：焦绿石型氧化钨；钨酸铵溶液；亚铁离子；结晶；机理

(Edited by Xiang-qun LI)